A molecularly Imprinted Electrochemical Sensor Based on N-MWCNT/CPE for Highly Sensitive and Selective Detection of Bisphenol A

Ruli Xu[1], Xiaomin Qian[2], Zhiyuan Zhang[1], Fanshu Yuan[1], Yuqing Song[1], Jie Liu[1], Qianli Zhang[1,], Jie Wei[1,*]*

[1] School of chemistry and life Science, Suzhou University of Science and Technology, 1 Kerui Road, Suzhou 215011, China
[2] WuJiang Center for Disease Control and Prevention, WuJiang Public Health Center, 551 GaoXin Road, Suzhou 215200, China
[*]E-mail: zqlmhb@163.com (Q. Zhang) ustsweijie@163.com (J. Wei)

A sensitive and selective carbon paste electrode (CPE) for the detection of bisphenol A (BPA) was prepared using N doped multi-walled carbon nanotubes (N-MWCNT) as the electron transport accelerator and molecularly imprinted polymer (MIP) as the recognition element of BPA. In presence of the initiator of 2, 2′-azobis(isobutyronitrile) (AIBN), BPA was imprinted using acrylonitrile as a functional monomer and ethylene glycol dimethacrylate (EGDMA) as a cross-linker. The polymers of MIP and non-molecularly imprinted polymer (NIP) were characterized by Fourier transform infrared spectroscopy (FT-IR) and scanning electron microscopy (SEM). Under the optimized conditions, the oxidation peak current increases linearly with the increase of BPA concentration in the range of 0.05 – 90 µmol/L (R = 0.9991), and the detection limit was 11.8 nmol/L. MIP/N-MWCNT/CPE successfully detected BPA in the elution solution of a plastic bottle.

1. INTRODUCTION

BPA, a produced chemical monomer, is widely used as an intermediate for plasticizing, binding, or hardening plastics. Furthermore, BPA can also act as both a substrate for the production of polycarbonate resin and an additive for thermal paper and flame-retardants [1,2]. The consumption of BPA increases sharply because of the increasing demand of the polycarbonate. The polycarbonate product is everywhere in life, such as automotive applications, optical media, can linings, water supply

pipelines, beverage packaging, medical devices, baby bottles, and other daily necessities. Thus, the emission of BPA to air, surface water, and soil are severe pollution during the related manufacture and the utilization of BPA containing products [3].

BPA is an endocrine disrupting compound. The phenol groups in BPA is similar to those in estradiol and diethylstilbestrol, and they are easy to bind to estrogen receptors [4]. BPA can severely damage people's immune systems and lead to endocrine disorders [5]. In addition, long-term exposure to BPA can cause reproductive organs, thyroid, and brain abnormalities, resulting in obesity, neurotoxicity, cardiovascular diseases and child developmental problems [6,7]. Many counties identify BPA as a toxic chemical. European Union proclaimed that the secure concentration of BPA in water should below 1.5 mg/L. Hence, it is necessary to explore a simple, rapid, sensitive and selective method for BPA detection to control the exposure and potential health effects.

Recently, BPA was detected by various analytical methods including high performance liquid chromatography (HPLC) [8,9], gas chromatography-mass spectrometry (GC-MS) [10,11], enzyme-linked immunosorbent assay (ELISA) [12], fluorescence [13,14], and chemiluminescence [15]. Compared with the mentioned methods, electrochemical sensor owns unique advantages, such as simplicity, low-cost, excellent sensitivity and high analysis speed. Various nanomaterials modified electrodes were explored for the BPA detection [16-19]. For example, Huang and coworkers [20] reported a portable 3D-printed electrochemical electrode for the detection of BPA based on a covalent organic framework (COF DQTP)-modified pencil graphite electrode (DQTP/PGE). The linearity range was 0.5-30 μmol/L and a detection limit of 0.15 μmol/L (S/N = 3). Baghayeri and coworkers [21] reported a voltammetric aptamer sensor for the BPA detection by an MWCNT/Fe_3O_4@gold nanocomposite. The linear response was in the range of 0.1 – 8 nmol/L and had a detection limit of 0.03 nmol/L.

Molecular imprinting technology is a method to obtain the target adsorption and detection [22,23]. MIP is usually prepared via the polymerization of a monomer in the presence of the template. After removing the template, MIP owns the binding sites complementing the target in shape, size and function. MIP is used in various fields, such as drug delivery, sample pretreatment, contaminant removal, and sensor technology due to MIP's advantages of excellent recognition and stability. Combining the merits of MIP and nano-materials, MIP based electrochemical sensors have been reported for the sensitive and selective detection of pollutions [24-27].

Herein, N-doped MWCNT was used to enhance the electrochemical sensor's sensitivity because of its rich edge sites and high electric conductivity [28]. Moreover, the bonding configuration of N atoms on the surface of MCNT can improve the electrocatalytic properties. BPA was imprinted by bulk polymerization with a functional monomer of acrylonitrile, a cross-linker of EGDMA and the initiator of AIBN. After removing BPA, MIP combined with N-MWCNT was used as the modified materials of carbon paste electrode for BPA detection. This established method has been used to detect BPA in the elution solution of a plastic bottle with satisfied recoveries.

2. EXPERIMENTAL SECTION

2.1. Materials and reagents

Ethylene glycol dimethacrylate (EGDMA), 2, 2′-azobis(isobutyronitrile) (AIBN), acrylonitrile, bisphenol A, tetrabromo bisphenol (TBBPA), hydroquinone, catechol, and p-nitrophenol were purchased from Aladdin, Shanghai. Carbon powder, mineral oil, KH_2PO_4, Na_2HPO_4, ethanol and acetic acid were supplied by Sinopharm Chemical Reagent Co., Ltd. N doped multi-walled carbon nanotubes(N-MWCNT) was obtained from Nanjing XFNANO Materials Tech Co., Ltd. The reagents were used without further purification.

2.2. Characterization and electrochemical determinations

Fourier transform infrared spectrometer (FT-IR) was conducted using KBr pellets on a Spectrum BXII spectrometer (Perkin Elmer, America). The morphology was studied with field emission scanning electron microscopy (FESEM) using a ZEISS Gemini 300 instrument. The electrochemical determinations were carried out on an RST5000 electrochemical workstation (Suzhou, China) with a three-electrode system with a modified CPE as the working electrode, a platinum wire as the counter electrode, and an Ag/AgCl as the reference electrode. The electrochemical determinations were carried out on an RST5000 electrochemical workstation (Suzhou, China) using a three-electrode system of a modified CPE as the working electrode, a platinum wire as the counter electrode, and an Ag/AgCl as the reference electrode.

2.3. Synthesis of MIP

The mixture of 1 mmol BPA, 3 mmol acrylonitrile and 30 mL ethanol was ultrasonic for 20 min and then added with 12 mmol EGDMA and 0.3 mmol AIBN. The polymerization reaction was implemented under nitrogen protection at 60°C for 24 h. The BPA template was removed by the Soxhlet extractor method using the extract solution of methanol/acetic acid=7:3. MIPs were washed using ethanol and vacuum drying at 60°C. For comparison, the preparation of non-imprinted polymers (NIPs) was prepared under the same conditions except for the addition of the BPA template.

2.4. Fabrication of molecularly imprinted electrochemical sensor

N-MWCNT was activated by refluxing in concentrated HCl at 100°C for 12 h. N-MWCNT was washed with deionized water to pH 7.0, and vacuum dried at 110°C for 12 h.

40 mg MIP was mixed fully with 20 mg N-MWCNT, 220 mg graphite powder and 120 mg methyl silicone oil in an agate mortar. And then, the paste was tightly filled into a CPE mold (3.0 mm in diameter) to fabricate a MIP electrochemical sensor (MIP/N-MWCNT/CPE). The electrode surface was smoothed with a weighing paper. A NIP electrochemical sensor (NIP/N-MWCNT/CPE) was obtained following a similar procedure with the addition of NIP.

2.5. Pretreatment of actual samples

    5 g plastic bottle sample (polycarbonate) was cut into small rectangular pieces with scissors, washed with deionized water, and then placed in PBS (pH 7.0) solution (30 mL), soaked for 30 days, finally evaporated to concentrate by heating. Taking 100 μL of the concentrate and put it into 10 mL of PBS (pH = 7.0) solution for electrochemical detection.

3. RESULTS AND DISCUSSION

3.1. The characterization of MIP and NIP

    MIP (BPA eluted) and NIP were characterized by infrared spectroscopy to elucidate the formation of polymer (Fig. 1). For MIP, the absorption peak at 2239 cm^{-1} is caused by the stretching vibration of the nitrile group (-C≡N). The bands at 2940 cm^{-1}, 1450 cm^{-1} and 1369 cm^{-1} are mainly attributed to the stretching vibrations, bending vibrations and swinging vibration of methylene, respectively. Sharp band at 1725 cm^{-1} corresponds to the stretching vibration of carbonyl group (-C=O) [29]. Moreover, the peak at 1125 cm^{-1} is due to the contribution of the CO–O peak. The FT-IR spectrum of NIP is similar with that of MIP (BPA eluted). The adsorption band at 3325 cm^{-1} related to -OH group in BPA is found to be disappeared in the FT-IR spectrum of MIP (BPA eluted). The adsorption band at 3325 cm^{-1} related to -OH group in BPA is found to be disappeared in the FT-IR spectrum of MIP (BPA eluted) or NIP. Which were similar to Zhang et al. [30] results: The BPA did not exist in NIP, which was the fundamental difference between MIP and NIP. Thus, molecularly imprinted polymer for BPA is prepared successfully by the thermal polymerization process.
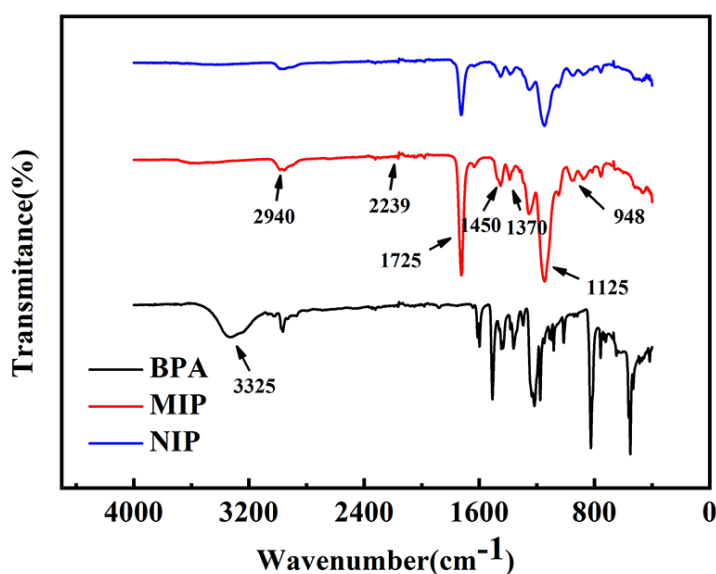
Figure 1. FT-IR spectra of NIP (blue line), BPA removed -MIP (red line) and BPA (black line) as a reference material.

The morphology of the polymers was investigated by SEM. Figure 2 gives the SEM image of MIP (Figure 2 A and B) and NIP (Figure C and D) at different magnification. MIP and NIP show agglomerates of nanosize globules, which were similar to the previous report [31]. MIP is consisted of ~600 nm globules, while NIP is composed of ~100 nm globules. The template molecule can influence the nucleation, the polymer development confirmation, and the agglomeration degree [32]. Thus, the presence of BPA affects the particle size of MIP and NIP. It was also investigated that MIP had more surface roughness and depression places, which was in agreement with the observation by Vu [33]. As clearly shown in micrographs, imprinting technique created pores on the surface of the polymers.
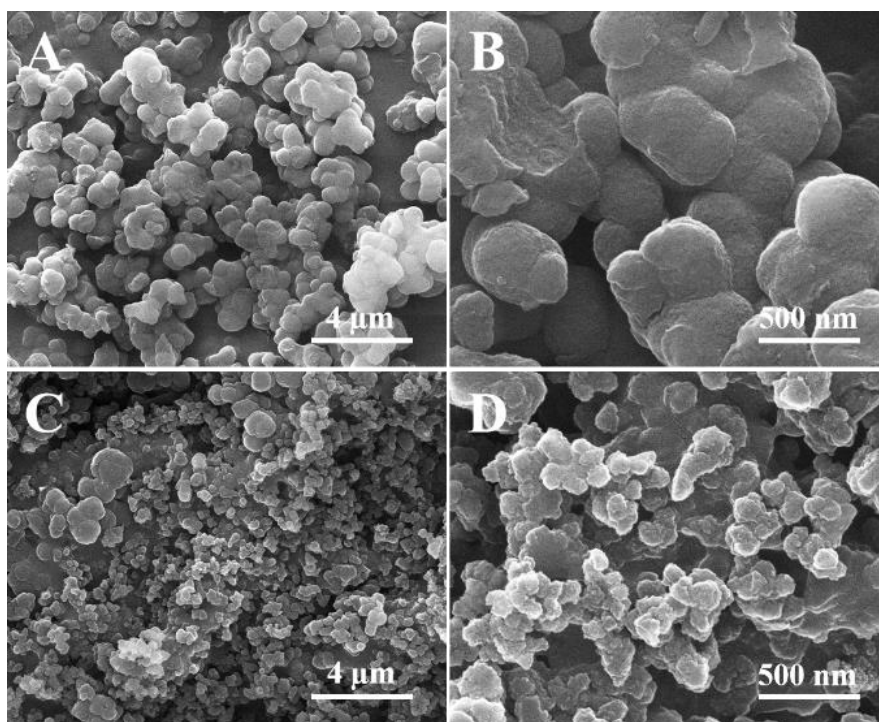
Figure 2. SEM image of BPA removed -MIP (A and B) and NIP (C and D) at different magnification.

3.2. Electrochemical behavior

Figure 3 showed CV curves of different electrodes in 20 mmol/L BPA. The BPA irreversible oxidation peak is clearly found at 0.58 V vs Ag/AgCl, which is near to BPA's oxidation potential of 0.62 V vs Ag/AgCl reported by Jalilian, et al [27].
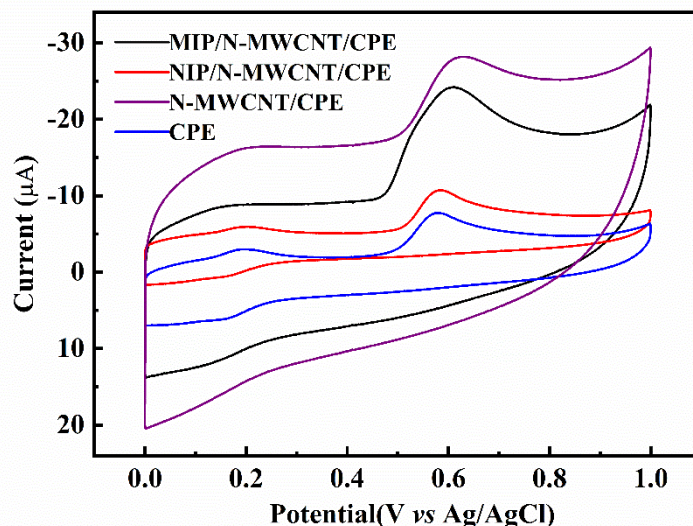
Figure 3. Cyclic voltammograms of 0.1 mol/L PBS (pH 7.00) containing 20 μmol/L BPA on CPE (blue curve), N-MWCNT/CPE (purple curve), MIP/N-MWCNT/CPE (black curve), and NIP/N-MWCNT/CPE (read curve). Scanning rate: 50 mV/s.

The oxidation current was 10.56 mA at N-MWCNT/CPE, approximately two times as much as that at the bare CPE (5.26 mA). This benefits from the increase of active area and the efficiency of electron transmission at N-MWCNT/CPE. For MIP/N-MWCNT/CPE, no BPA oxidation peak was observed in 0.1 mol/L PBS (pH 7.00), indicating the completely removing BPA from MIP. Ipa of 20 μmol/L BPA was 14.26 mA at MIP/N-MWCNT/CPE, about three times higher than that at NIP/N-MWCNT/CPE (5.01 mA). The recognition of BPA was attributed to both the hydrogen bonding between the functional groups on MIP and BPA and rebinding sites on MIP matching with the size and structure of BPA. The low current of BPA at NIP/N-MWCNT/CPE is due to the limited electron transferability of the polymer membrane.

3.3. Optimization of experimental conditions

Methyl silicone oil was controlled at 30% according to our previous work [34]. The effect of N-MWCNT and MIP was investigated using CV response in 0.1 mol/L PBS (pH 7.00) containing 20 μmol/L BPA. The current response increases rapidly in the ratio of N-MWCNT increase from 5% to 10%. As shown in Figure 4A, the oxidation peak current of BPA increases gradually when the ratio of MIP is in the range of 2% - 10%, and the current decrease slightly when the ratio of MIP is above 10%. The sites for adsorption of BPA increased with the increase of MIP in the modified electrode. However, excessive MIP affects the conductivity of the electrode. A similar phenomenon was found in 17 β-estradiol detection using a MIP electrochemical sensor based on MOF/CNT and Prussian blue. The ratio of both N-WCNT and MIP was optimized as 10% to prepare the electrochemical sensor in this work.

The effect of pH value on the BPA electrochemical performance was studied in the range of 6.0 – 8.0 (Figure 4B). The peak current conversely increased when pH increased from 6.0 to 7.0. The

dissociation state of BPA was greatly affected by the pH value of buffer solution. The pKa of BPA was 9.73 [35]. The maximum current response was obtained at pH 7.00, showing that MIP was more suitable for recognizing BPA in a non-dissociated state than in the dissociated state.
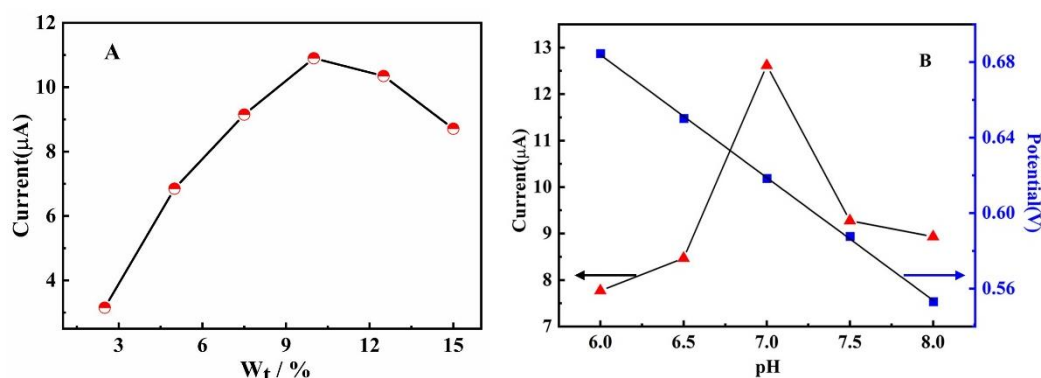

Figure 4. (A) The effect of the amount of BPA removed-MIP on the oxidation peak current of BPA. (B) The effect of pH value on the peak current and potential of BPA. Solution: 0.1 mol/L PBS (pH 7.00) containing 20 μmol/L BPA; Scanning rate: 50 mV/s.

Hence, 0.1 mol/L PBS of pH 7.00 was chosen in the electrochemical experiments. The oxidation peak potential linearly shifted to negative potential with the increase of pH value. The relationship between the oxidation peak potential of BPA and pH follows the equation of E_{pa} (V) = -0.065 pH + 1.074 (R=0.9899). Hence, the protons participate in the electrochemical oxidation of BPA. The slope of 65 mV/pH was near 59 mV/pH, illustrating that the number of transfer electrons keeps in line with the number of involved protons. The linear relationship between oxidation potential of BPA and pH was also reported in cobalt phthalocyanine modified carbon paste electrode for BPA detection [36].

The effect of incubation time on the oxidation peak current of BPA was investigated using 0.1 mol/L PBS (pH 7.00) containing 20 mmol/L BPA. As shown in Figure 5A, the oxidation peak current of BPA gradually increased when the incubation time was in the range of 60 – 300 s, and then reached a platform when the incubation time was above 300 s. This phenomenon resulted from the amount of BPA initially increased, and then supersaturation on the electrode surface. So, the optimized incubation time was 300 s.

The effect of scan rate was studied to acquire some information about the electrochemical mechanism. Figure 5B gives the relationship between the peak current and scan rate. The oxidation peak current increases linearly with the square root of scan rate and obey the following equation: I_{pa} (μA) $=2.06 \, \nu^{1/2}$ (mV/s)$^{1/2}$ – 5.661 (R = 0.9956). It proves that the oxidation of BPA on MIP/N-MWCNT/CPE is a diffusion control process. In this work, 50 mV/s was chosen in the further experiment.
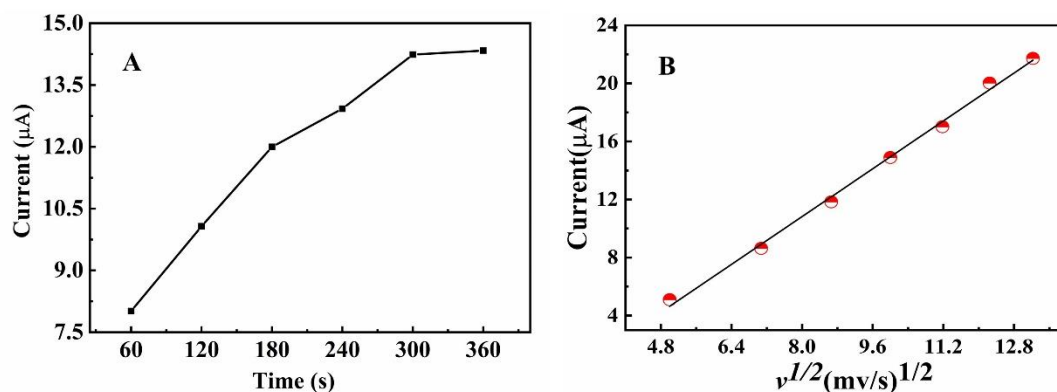
Figure 5. The effect of incubation time (A) and scan rate (B) on the oxidation peak current of BPA. The other conditions were the same as Figure 4.

3.4. Calibration curve

The detection range and detection limit of MIP/N-MCNT/CPE for BPA were studied by CV (Figure 6). The oxidation current gradually increases with the concentration of BPA and exhibits a perfect linear relationship in the range of 0.05 – 90 µmol/L. The linear equation was *Ip* (µA) = -0.063+ 1.68*C* (R = 0.9991). The detection limit was 11.8 nmol/L (S/N = 3). The comparison of this work with other reported BPA electrochemical sensors is listed in Table 1, which betoken that MIP/N-MCNT/CPE meets the requirement of the determination of BPA in real samples.
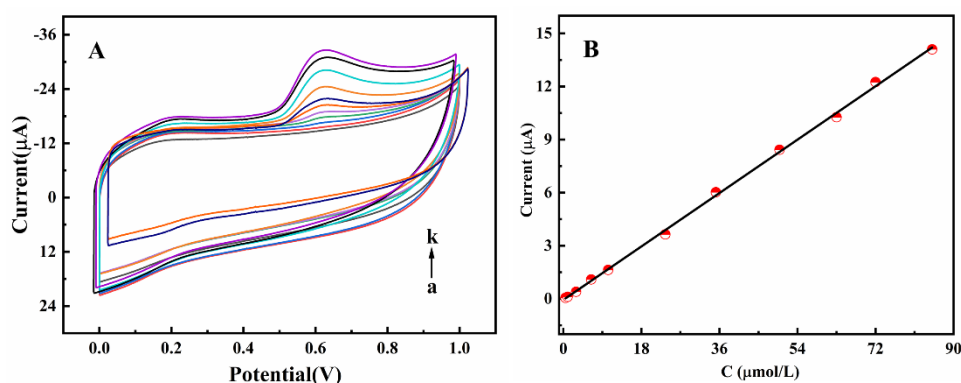
Figure 6. (A) The CV curves of different BPA concentration using MIP/N-MCNT/CPE, a-k: 0.05, 1.0, 2.9, 6.4, 10.3, 23.5, 35.2, 50.0, 63.7 and 85.1 µmol/L. (B) The linear plot between peak current and BPA concentration. Other conditions were same as Figure 4.

Table 1. Comparison of different electrodes for the determination of BPA

Electrode	Linear range (µmol/L)	LOD (µmol/L)	Reference
MIP-AuNPs-MCA-rGO/CILE	0.004 - 18	0.001	[27]
MIP/LSG	0.05 - 20	0.008	[37]
MIP/B,N,F-CQDs/AgNPs /GCE	0.01 - 50	0.01	[38]
MIP/AuNPs/CS/GCE	0.015 - 55	0.001	[39]
MIP/MWCNT/GCE	0.2 - 45	0.03	[40]
MIP-MWCNTs/CPE	0.05 - 90	0.01	This work

AuNPs – Au nanoparticles; MCA – mercaptamine; rGO – reduced graphene oxide; CILE - carbon ionic liquid electrode; LSG - laser scribed graphene; CQDs – carbon quantum dots; AgNPs – Ag nanoparticles; GCE – glass carbon electrode; CS – chitosan.

3.5. Interference studies

Tetrabromo bisphenol A (TBBPA), hydroquinone, catechol and p-Nitrophenol were chosen as the competitors to elucidate the selective recognition ability of MIP/N-MCNT/CPE. They have similar structures and functional groups. The electrochemical signals of MIP/N-MCNT/CPE in 0.1 mol/L PBS containing 20 µmol/L BPA were recorded in the presence of 200-fold hydroquinone, catechol and p-Nitrophenol, and 50-fold TBBPA. As shown in Figure 7, such interferents has little effect on the determination of BPA. Moreover, 500-fold methanol, ethanol, K^+ or Na^+ were also investigated. There is no impact on the oxidation of BPA. Similar experiments were conducted using NIP/N-MCNT/CPE. The oxidation peak current changed obviously under such competitors on NIP/N-MCNT/CPE. These phenomena indicate the excellent selectivity of MIP/N-MCNT/CPE.
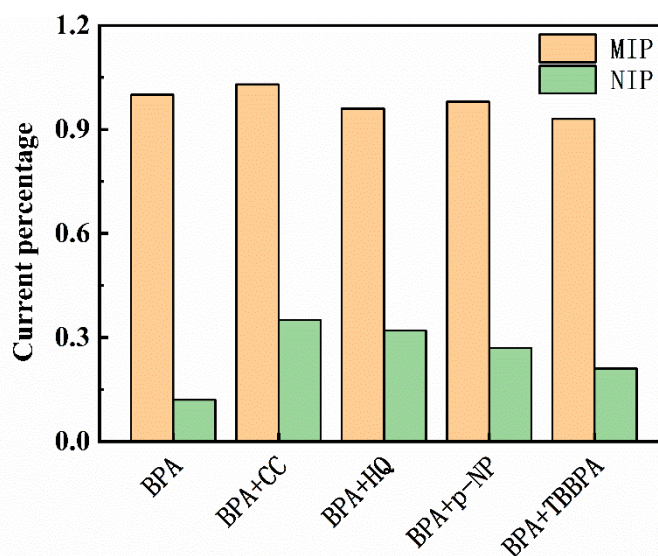
Figure 7. Column graph of CV signals in 20 µmol/L BPA and the analogues (200-fold hydroquinone, catechol and p-Nitrophenol, and 50-fold TBBPA). Other conditions were the same as Figure 4.

3.6. Stability and Reproducibility

Excellent stability and reproducibility were significant for the electrochemical sensor in practical application. Kept in a refrigerator for around 30 days, MIP/N-MCNT/CPE was used for BPA detection once every five days. The oxidation peak currents of 50 mmol/L BPA changed little. After 30 days, the current was 92.4% of the initial value, showing the terrific durability of MIP/N-MCNT/CPE. Five MIP/N-MCNT/CPE electrodes were prepared respectively based on the same procedure to evaluate the reproducibility of electrodes. RSD % was 3.25%. The regeneration of MIP/N-MCNT/CPE was carried out by cutting off a layer of carbon paste on the surface of the electrode and polishing it on a smooth paper. RSD% of six repeated determinations using a new electrode was 2.68%. The results testified that the reproducibility of MIP/N-MCNT/CPEs was perfect.

3.7. Sample analysis

Table 2. Determination of BPA in plastic bottle leaching solution

Sample No.	Determined (μmol/L)	Added (μmol/L)	Total found (μmol/L)	Recovery(%)
1	1.86	5.00	6.68	97.38
		10.00	11.80	99.50
		15.00	17.12	103.54
2	2.05	5.00	6.98	99.00
		10.00	12.02	99.75
		15.00	17.15	100.59
3	1.96	5.00	6.87	98.70
		10.00	11.55	96.57
		15.00	16.54	97.52

The pieces of a plastic bottle were soaked in PBS buffer (pH 7.0) for 30 days. BPA in the sample was leached and detected by MIP/N-MCNT/CPEs under the optimized experimental conditions. The concentration of BPA was 1.96 μmol/L in the leaching solution (n=3). The recovery test of BPA was performed. As found in table 2, the recovery was in the range of 97.32% – 103.54%, proving that the established electrochemical sensor owned delightful accuracy for the sample detection.

4. CONCLUSION

BPA was detected by a MIP/N-MWCNT/CPE, in which N-MWCNT plays a role in accelerating electron transfer and improving electrode sensitivity. MIP was used to enhance the molecular recognizing ability of the electrochemical sensor. The advantages of MIP/N-MCNT/CPE include a wide linear range, a low detection limit, perfect stability and reproducibility, and high selectivity. Moreover, the constructed method was used to successfully detect BPA in the elution solution of a plastic bottle

with satisfactory recoveries. This strategy is hopeful for exploring other electrochemical sensors for other environmental pollutions.

References

1. M. F. Fernandez, J. P. Arrebola, J. Taoufiki, A. Navalon, O. Ballesteros, R. Pulgar, J. L. Vilchez, N. Olea, *Reprod Toxicol,* 24(2007)259.
2. Xu, Y. Du, L. Liu, D. Fan, L. Yan, X. Liu, H. Wang, Q. Wei, H. Ju, *Sensor Actuat. B: Chem.,* 330(2021)129387.
3. M. Murugananthan, S. Yoshihara, T. Rakuma, T. Shirakashi, *J. Hazard. Mater.,* 154(2008)213.
4. A. U. Alam, M. J. Deen, *Anal. Chem.,* 92(2020)5532.
5. Y. Tian, P. Deng, Y. Wu, J. Li, J. Liu, G. Li, Q. He, *J. Electrochem. Soc.,* 167(2020)046514.
6. B. S. Rubin, *J. Steroid Biochem.,* 127(2011)27.
7. J.T. Wolstenholme, E. F. Rissman, J. J. Connelly, *Horm. Behav.,* 59(2011)296.
8. M. A. Gross, S. G. C. Moreira, M. A. Pereira-da-Silva, F. F. Sodre, L. G. Paterno, *Sci. Total Environ.,* 763(2021)142985.
9. N. P. Kalogiouri, A. Pritsa, A. K abir, K. G. Furton, V. F. Samanidou, *J. Sep. Sci.,* 44(2021)1633.
10. N. Subuhi, S. M. Saad, N. N. M. Zain, V. Lim, M. Miskam, S. Kamaruzaman, M. Raoov, N. Yahaya, *J. Sep. Sci.,* 43(2020)3294.
11. A. Azzouz, L. P. Colon, L. Hejji, E. Ballesteros, *Anal. Bioanal. Chem.,* 412(2020)2621.
12. M. Jia, S. Chen, T. Shi, C. Li, Y. Wang, H. Zhang, *Food Chem.,* 344(2021)128602.
13. L. Zeng, X. Zhang, X. Wang, D. Cheng, R. Li, B. Han, M. Wu, Z. Zhuang, A. Ren, Y. Zhou, T. Jing, *Biosens. Bioelectron.,* 180(2021)113106.
14. C. W. Chuang, W. S. Huang, H. S. Chen, L. F. Hsu, Y. Y. Liu, T. C. Chen, *Int J Environ. Res. Public Health.,* 18(2021)1102.
15. Y. Xiong, Q. Wang, M. Duan, J. Xu, J. Chen, S. Fang, *Polymers,* 10(2018)780.
16. M. Malakootian, S. Hamzeh, H. Mahmoudi-Moghaddam, *Electroanal.,* 33(2020)38.
17. N. A. Azis, I. M. Isa, N. Hashim, M. S. Ahmad, S. N. A. M. Yazid, M. I. Saidin, S. M. Si, R. Zainul, A. Ulianas, S. Mukdasai, *Int. J. Electrochem. Sc.,* 14(2019)10607.
18. C. Li, Y. Zhou, X. Zhu, B. Ye, M. Xu, *Int. J. Electrochem. Sc.,* 13(2018)4855.
19. N. S. M. Rais, I. M. Isa, N. Hashim, M. I. Saidin, S. N. A. M. Yazid, Ahmad, M. S. Mukdasai, S *Int. J. Electrochem. Sc.,* 14(2019)7911.
20. Y. Y. Huang, Y. H. Pang, X. F. Shen, R. Jiang, Y. Y. Wang, *Talanta,* 236(2022)122859.
21. M. Baghayeri, R. Ansari, M. Nodehi, I. Razavipanah, H. Veisi, *Microchim. Acta,* 185(2018)320.
22. G. Zhang, M. M. Ali, X. Feng, J. Zhou, L. Hu, *TRAC Trend. Anal. Chem.,* 144(2021)116426.
23. Y. Xu, T. Huang, S. Wang, M. Meng, Y. Yan, *J. Environ. Chem. Eng.,* 10(2022)106850.
24. K. Glosz, A. Stolarczyk, T. Jarosz, *Materials,* 14(2021)1369.
25. A. M. Santos, A. Wong, T. M. Prado, E. L. Fava, O. Fatibello-Filho, M. Sotomayor, F. C. Moraes, *Talanta,* 224(2021)121804.
26. M. Mehmandoust, N. Erk, C. Karaman, O. Karaman, *Chemosphere,* 291(2021)132807.
27. R. Jalilian, E. Ezzatzadeh, A. Taheri, *J. Environ. Chem. Eng.,* 9(2021)105513.
28. X. Xin, S. Sun, M. Wang, R. Jia, *Ionics,* 26(2019)2633.
29. H. L. Wu, D. H. Bremner, H. Y. Li, Q. Q. Shi, J. Z. Wu, R. Q. Xiao, L. M. Zhu, *Mater. Sci. Eng. C Mater. Biol. Appl.,* 62(2016)702.
30. Y. Zhang, W. Huang, X. Yin, K. A.Sarpong, L. Zhang, Y. Li, S. Zhao, H. Zhou, W. Yang, W. Xu,

React. Funct Polym., 157 (2020)104767.
31. P. Karthika, S. Shanmuganathan, S. Viswanathan, C. Delerue-Matos, *Food Chem.*, 363(2021)130287.
32. S. Rebocho, C. M. Cordas, R. Viveiros, T. Casimiro, *J. Supercrit. Fluid*, 135(2018)98.
33. V. P. Vu, Q. T. Tran, D. T. Pham, P. D. Tran, B. Thierry, T. X. Chu, A. T. Mai, *Vietnam J. Chem.*, *57*(2019) 328.
34. M. Zhu, R. Xu, X. Wang, J. Liu, Q. Zhang, J. Wei, *Int. J. Electrochem. Sc.,* 16(2021)211228.
35. H. Sambe, K. Hoshina, K. Hosoya, J. Haginaka, *J. Chromatogr. A*, 1134(2006)16.
36. H.-s. Yin, Y.-l. Zhou, S.-y. Ai, *J. Electroanal. Chem.*, 626(2009)80.
37. T. Beduk, A. Ait Lahcen, N. Tashkandi, K. N. Salama, *Sensor Actuat. B: Chem.*, 314(2020)128026.
38. J. Yao, M. Chen, N. Li, C. Liu, M. Yang, *Anal. Chim. Acta*, 1066(2019)36.
39. W.-R. Zhao, T.-F. Kang, L.-P. Lu, F.-X. Shen, S.-Y. Cheng, *J. Electroanal. Chem.*, 786(2017)102.
40. B. Liu, J. Yan, M. Wang, X. Wu, *Int. J. Electrochem. Sc.*, 14(2019)3610.